A Data-Driven Transcriptional Taxonomy of Adipogenic Chemicals to Identify White and Brite Adipogens

Stephanie Kim,*[1,2,] Eric Reed,*[1,3,4] Stefano Monti,[#1,3,4] Jennifer Schlezinger[#1,2]

*Co-first authors

[#]Co-senior authors

[1]Boston University Superfund Research Program, Boston University, MA 02118 USA

[2]Boston University School of Public Health, Department of Environmental Health, MA 02118 USA

[3]Boston University School of Medicine, Department of Computational Medicine, MA 02118 USA

[4]Boston University Bioinformatics Program, MA 02115, USA

Corresponding author:
Jennifer J. Schlezinger, Ph.D.
Boston University School of Public Health
Dept. of Environmental Health
715 Albany Street, R-405
Boston, MA 02118
Phone: 617-358-1708
Email: jschlezi@bu.edu

Running Title:
Classification Taxonomy for Adipogenic Chemicals

Acknowledgements:

Declaration of competing financial interests (CFI):
The authors declare they have no actual or potential competing financial interests.

Grant Information:

Superfund Research Program [P42 ES007381]
BU-Joslin Pilot & Feasibility Program Award (2016)

Abstract:

Background: Chemicals in disparate structural classes activate specific subsets of PPARγ's transcriptional programs to generate adipocytes with distinct phenotypes.

Objectives: Our objectives were to 1) establish a novel classification method to predict PPARγ ligands and modifying chemicals, and 2) create a taxonomy to group chemicals based on their effects on PPARγ's transcriptome and downstream metabolic functions. We tested the hypothesis that environmental ligands highly ranked by the taxonomy, but segregated from therapeutic ligands, would induce white but not brite adipogenesis.

Methods: 3T3-L1 cells were differentiated in the presence of 76 chemicals (negative controls, nuclear receptor ligands known to influence adipocyte biology, suspected environmental PPARγ ligands). Differentiation was assessed by measuring lipid accumulation. mRNA expression was determined by highly multiplexed RNA-Seq and validated by RT-qPCR. A novel classification model was developed using an amended random forest procedure. A subset of environmental contaminants identified as strong PPARγ agonists were analyzed by their effects on lipid handling, mitochondrial biogenesis and cellular respiration in 3T3-L1 cells and human preadipocytes.

Results: We used lipid accumulation and RNA sequencing data to develop a classification system that 1) identified PPARγ agonists, and 2) sorted agonists into likely white or brite adipogens. Expression of *Cidec* was the most efficacious indicator of strong PPARγ activation. Two known environmental PPARγ ligands, tetrabromobisphenol A and triphenyl phosphate, which sorted distinctly from therapeutic ligands, induced white but not brite adipocyte genes and induced fatty acid uptake but not mitochondrial biogenesis in 3T3-L1 cells. Moreover, two chemicals identified as highly ranked PPARγ agonists, tonalide and quinoxyfen, induced white

adipogenesis without the concomitant health-promoting characteristics of brite adipocytes in mouse and human preadipocytes.

Discussion: A novel classification procedure accurately identified environmental chemicals as PPARγ ligands distinct from known PPARγ-activating therapeutics. The computational and experimental framework has general applicability to the classification of as-yet uncharacterized chemicals.

Introduction:

Since 1980, the prevalence of obesity has been increasing globally and has doubled in more than 70 countries. In 2015, it was estimated that a total of 108 million children and 604 million adults were obese worldwide (GBD 2017). This poses a major public health threat since overweight and obesity increase the risk of metabolic syndrome, which, in turn, sets the stage for metabolic diseases, such as type 2 diabetes, cardiovascular disease, nonalcoholic fatty liver disease and stroke (Park et al. 2003). The Endocrine Society's latest scientific statement on the obesity pathogenesis states that obesity is a disorder of the energy homeostasis system, rather than just a passive accumulation of adipose, and that environmental factors, including chemicals, confer obesity risk (Schwartz et al. 2017). The rapid increases in obesity and metabolic diseases correlate with substantial increases in environmental chemical production and exposures over the last few decades, and experimental evidence in animal models demonstrates the ability of a broad spectrum of various environmental metabolism-disrupting chemicals to induce adiposity and metabolic disruption (Heindel et al. 2017).

Adipocytes are crucial for maintaining metabolic homeostasis as they are repositories of free fatty acids and release hormones that can modulate body fat mass (Rosen and Spiegelman 2006). Adipogenesis is a highly regulated process that involves a network of transcription factors acting at different time points during differentiation (Farmer 2006). Peroxisome proliferator activated receptor γ (PPARγ) is a ligand activated, nuclear receptor and essential regulator of adipocyte formation and function (Tontonoz et al. 1994), as well as metabolic homeostasis, as all PPARγ haploinsufficient and KO models present with lack of adipocyte formation and metabolic disruption (Gumbilai et al. 2016; He et al. 2003; Jiang et al. 2014; O'Donnell et al. 2016; Zhang et al. 2004).

PPARγ activation regulates energy homeostasis by both stimulating storage of excess energy as lipids in white adipocytes and stimulating energy utilization by triggering mitochondrial biogenesis, fatty acid oxidation and thermogenesis in brite and brown adipocytes. The white adipogenic, brite/brown adipogenic and insulin sensitizing activities of PPARγ are regulated separately through post-translational modifications (Banks et al. 2015; Choi et al. 2010; Choi et al. 2011; Qiang et al. 2012) and differential co-regulator recruitment (Burgermeister et al. 2006; Feige et al. 2007; Ohno et al. 2012; Villanueva et al. 2013). Importantly, humans with minimal brite adipocyte populations are at higher risk for obesity and type 2 diabetes (Claussnitzer et al. 2015; Sidossis and Kajimura 2015; Timmons and Pedersen 2009).

Growing evidence supports the hypothesis that environmental PPARγ ligands induce phenotypically distinct adipocytes. Tributyltin (TBT) induces the formation of an adipocyte with reduced adiponectin expression and altered glucose homeostasis (Regnier et al. 2015). Furthermore, TBT fails to induce expression of genes associated with browning of adipocytes (e.g. *Ppara*, *Pgc1a*, *Cidea*, *Elovl3*, *Ucp1*) in differentiating 3T3-L1 adipocytes (Kim et al. 2018; Shoucri et al. 2018). As a result, TBT-induced adipocytes fail to up-regulate mitochondrial biogenesis and have low levels of cellular respiration (Kim et al. 2018; Shoucri et al. 2018). The structurally similar environmental PPARγ ligand, triphenyl phosphate, also fails to induce brite adipogenesis, and this correlates with an inability to prevent PPARγ from being phosphorylated at S273 (Kim et al. 2020).

The EPA developed the Toxicity Forecaster (ToxCast™) program to use high-throughput screening assays to prioritize chemicals and inform regulatory decisions regarding thousands of environmental chemicals (Kavlock et al. 2012). Several ToxCast™ assays can measure the

ability of chemicals to bind to or activate PPARγ, and these assays have been used to generate a toxicological priority index (ToxPi) that were expected to predict the adipogenic potential of chemicals in cell culture models (Auerbach et al. 2016). Yet, it has been shown that the results of ToxCast™ PPARγ assays do not always correlate well with activity measured in a laboratory setting and that the ToxPi designed for adipogenesis was prone to predicting false positives (Janesick et al. 2016). Furthermore, the ToxCast/ToxPi approach cannot distinguish between white and brite adipogens (Pereira-Fernandes et al. 2014).

In this study, we investigate differences in cellular response between adipogenic and non-adipogenic compounds, as well as the heterogeneity of response across adipogenic compounds. Our ultimate goal is the identification of potential novel adipogenic compounds, and the taxonomic organization of known and predicted adipogenic compounds based on their divergent transcriptional response. To this end, we generated phenotypic and transcriptomic data from adipocytes differentiated in the presence of 76 different chemicals. We combined the cost-effective generation of agonistic transcriptomic data by 3'Digital Gene Expression – a highly multiplexed RNA-Seq technology – with a new classification method to predict PPARγ-activating and modifying chemicals. Further, we investigated metabolic-related outcome pathways as effects of the chemical exposures. We created a data-driven taxonomy to specifically classify chemicals into distinct categories based on their various interactions with and effects on PPARγ. Based on the taxonomy-based predictions, we tested the phenotype (white *vs.* brite adipocyte functions) of environmental adipogens predicted to fail to induce brite adipogenesis in 3T3-L1 cells and primary human adipocytes.

Methods:

Chemicals

DMSO was purchased from American Bioanalytical (Natick, MA). CAS numbers, sources and catalog numbers of experimental chemicals are provided in **Table S1**. Human insulin, dexamethasone, 3-isobutyl-1-methylxanthine (IBMX), and all other chemicals were from Sigma-Aldrich (St. Louis, MO) unless noted.

Cell Culture

NIH 3T3-L1 (ATCC: CL-173, RRID:CVCL_0123, Lot # 63343749) pre-adipocytes were maintained in Growth Medium (high-glucose DMEM with 10% calf serum, 100 U/ml penicillin, 100 μg/ml streptomycin, 0.25 μg/ml amphotericin B). All experiments were conducted with cells between passages 3 and 8. Experimental conditions are outlined in **Table 1** and **Figure S1A**. For experiments, cells were plated in Growth Medium and incubated for 4 days, at which time the cultures are confluent for 2 days. "Naïve" pre-adipocytes were cultured in Growth Medium for the duration of an experiment. On day 0, differentiation was induced by replacing the medium with Differentiation Medium (DMEM,10% fetal bovine serum (FBS, Sigma-Aldrich), 100 U/ml penicillin, 100 μg/ml streptomycin, 250 nM dexamethasone, 167 nM human insulin, 0.5 mM IBMX). Also on day 0, single experimental wells were treated with vehicle (DMSO, 0.2% final concentration), rosiglitazone (positive control, 100 nM) or test chemicals. On days 3 and 5 of differentiation, medium was replaced with Maintenance Medium (DMEM, 10% FBS, 167 nM human insulin, 100 U/ml penicillin, 100 μg/ml streptomycin), and the cultures were re-dosed. On Day 7 of differentiation, medium was replaced with Adipocyte Medium (DMEM, 10% FBS, 100 U/ml penicillin, 100 μg/ml streptomycin), and the cultures were re-dosed. On day 10, cytotoxicity was assessed by microscopic inspection, with cultures containing more than 10% rounded cells excluded from consideration (See **Table S1** for information on maximum

concentrations tested). Wells with healthy cells were harvested for analysis of gene expression, lipid accumulation, fatty acid uptake, mitochondrial biogenesis, mitochondrial membrane potential, and cellular respiration.

Primary human subcutaneous pre-adipocytes were obtained from the Boston Nutrition Obesity Research Center (Boston, MA) and differentiated as previously described (Lee and Fried 2014). Experimental conditions are outlined in **Table 1** and **Figure S1B**. The pre-adipocytes were maintained in Growth Medium (αMEM with 10% FBS, 100 U/ml penicillin, 100 µg/ml streptomycin, 0.25 µg/ml amphotericin B). For experiments, human pre-adipocytes were plated in Growth Medium and grown to confluence (3-5) days. "Naïve" pre-adipocytes were cultured in Growth Medium for the duration of an experiment. On day 0, differentiation was induced by replacing the Growth Medium with Differentiation Medium (DMEM/F12, 25 mM $NaHCO_3$, 100 U/ml penicillin, 100 µg/ml streptomycin, 33 µM d-Biotin, 17 µM pantothenate, 100 nM dexamethasone, 100 nM human insulin, 0.5 mM IBMX, 2 nM T_3, 10 µg/ml transferrin). Also on day 0, single experimental wells also were treated with vehicle (DMSO, 0.1% final concentration), rosiglitazone (positive control, 4 µM) or test chemicals. On day 3 of differentiation, medium was replaced with fresh Differentiation Medium, and the cultures were re-dosed. On days 5, 7, 10, and 12 of differentiation, the medium was replaced with Maintenance Medium (DMEM/F12, 25 mM $NaHCO_3$, 100 U/ml penicillin, 100 µg/ml streptomycin, 3% FBS, 33 µM d-Biotin, 17 µM pantothenate, 10 nM dexamethasone, 10 nM insulin), and the cultures were re-dosed. Following 14 days of differentiation and dosing, cells were harvested for analysis of gene expression, lipid accumulation, fatty acid uptake, mitochondrial biogenesis, and cellular respiration.

Lipid Accumulation

3T3-L1 cells or human preadipocytes were plated in 24 well plates at 50,000 cells per well in 0.5 ml maintenance medium at initiation of the experiment. Dosing is outlined in **Table 1**. Medium was removed from the differentiated cells, and they were rinsed with PBS. The cells were then incubated with Nile Red (1 µg/ml in PBS) for 15 min in the dark. Fluorescence (λex= 485 nm, λem= 530 nm) was measured using a Synergy2 plate reader (BioTek Inc., Winooski, VT). The fluorescence in all experimental wells was normalized by subtracting the fluorescence measured in naïve pre-adipocyte cultures reported as "RFU."

Transcriptome Analysis

3T3-L1 cells were plated in 24 well plates at 50,000 cells per well in 0.5 ml maintenance medium at initiation of the experiment. Dosing is outlined in **Table 1**. Total RNA was extracted and genomic DNA was removed using the Direct-zol MagBead RNA Kit and following manufacturer's protocol (Zymo Research, Orange, CA). A final concentration of 5 ng RNA/ul was used for each sample. For each chemical, 3-5 replicates were profiled and carefully randomized across six 96-well plates, including 26 DMSO vehicle controls, and 16 naïve pre-adipocyte cultures. Sequencing and gene expression quantification was carried out by the MIT Technology Lab at Broad Institute (Cambridge, MA). RNA libraries were prepared using a highly multiplexed 3' Digital Gene Expression (3' DGE) protocol developed by (Xiong et al. 2017) and sequenced on an Illumina NextSeq 500, generating between 2.13E8 and 3.87E8 reads and a mean of 3.02E8 reads per lane across 96 samples. All reads containing bases with Phred quality scores < Q10 were removed. The remaining reads were aligned to mouse reference genome, GRCm38, and counted in 21,511 possible transcripts annotations. Only instances of uniquely aligned reads were quantified (i.e. reads that aligned to only one transcript). Furthermore, multiple reads with the same UMI, aligning to the same gene were quantified as a

single count. All processing and analyses of gene expression data were carried out in R (v 3.4.3). To reduce noise introduced by lowly quantified samples and genes, we performed quality control filtering procedures, which are described in detail in the Supplemental Material. Following sample- and gene-level quality control filtering, the final processed data set included expression levels of 9,616 genes for each of 234 samples. These 234 samples include 2-4 remaining replicates of each compound, 25 DMSO vehicle controls, and 15 naïve pre-adipocyte cultures.

PPARγ Ligand/Modifier Classification

A classification model was inferred from the *training set* consisting of 38 known PPARγ ligands or modifying compounds and 22 negative controls, including vehicle, to predict the label of the *test set* of 17 suspected PPARγ ligands/modifiers (**Table S1**). The model inference was based on an amended random forest procedure developed to better account for the presence of biological replicates in the data. The procedure is described in detail in the Supplemental Methods.

PPARγ Ligand/Modifier Clustering

Known and suspected PPARγ ligands/modifiers were clustered based on their test statistics from univariate analysis comparing each chemical or naïve pre-adipocyte exposure to vehicle using *limma* (v 3.34.9) (Ritchie et al. 2015). In order to assess taxonomic differences between different exposure outcomes, a recursive unsupervised procedure, which we denote as "K2 Taxonomer" (Reed et al., manuscript in preparation), was developed, whereby the set of PPARγ ligands/modifiers underwent recursive partitioning into subgroups. The procedure is described in detail in the Supplemental Materials.

Human Transcriptome Analysis

To assess the human relevance of the gene signatures derived from the PPARγ ligand/modifier clustering in chemical-exposed 3T3-L1 cells, we analyzed projections of these signatures onto the transcriptional profiles from 770 male subjects who were part of the Metabolic Syndrome in Men (METSIM) study. This publicly available data set, GEO accession number GSE70353 (Civelek et al. 2017), is comprised of microarray gene expression profiles from subcutaneous adipose tissue, as well as cardio-metabolic measurements. Affymetrix Human Genome U219 Array Microarray CEL files were annotated to unique Entrez gene IDs, using a custom CDF file from BrainArray (HGU219_Hs_ENSG_22.0.0). Each of the four possible gene sets derived from PPARγ ligand/modifier clustering were then projected on each of the 770 human transcriptome profiles using gene set variation analysis (GSVA), using *GSVA* (v 1.30.0) (Hanzelmann et al. 2013), resulting in an enrichment score for each gene set and sample.

For each projected gene set, we tested for relationships between single-sample enrichment scores and clinical measurements. Of notice, many of the clinical measurements are correlated with each other, such that confounding is likely to generate many spurious results. To overcome this problem, for each gene set projection, we tested the significance of the partial correlation between single-sample enrichment scores and each of the clinical variables while controlling for the remaining ones, including age, using the *ppcor* (v 1.1) R package. Given that the relationships between single-sample enrichment scores and any one clinical variable are not assumed to be linear, these partial correlations were calculated from Spearman correlation estimates. P-values were adjusted across all combinations of gene set and clinical measurement. Measurements with at least one comparison with a gene set projection yielding an FDR Q-value < 0.1 are reported. To reduce expected redundancies in the measurements, of the 23 initial

quantitative measurements included in these data, we ran this analysis on a subset of 12 measurements (**Table S2**).

Reverse Transcriptase (RT)-qPCR

3T3-L1 cells or human preadipocytes were plated in 24 well plates at 50,000 cells per well in 0.5 ml maintenance medium at initiation of the experiment. Dosing is outlined in **Table 1**. Total RNA was extracted and genomic DNA was removed using the 96-well Direct-zol MagBead RNA Kit (Zymo Research). cDNA was synthesized from total RNA using the iScript™ Reverse Transcription System (BioRad, Hercules, CA). All qPCR reactions were performed using the PowerUp™ SYBR Green Master Mix (Thermo Fisher Scientific, Waltham, MA). The qPCR reactions were performed using a 7500 Fast Real-Time PCR System (Applied Biosystems, Carlsbad, CA): UDG activation (50°C for 2 min), polymerase activation (95°C for 2 min), 40 cycles of denaturation (95°C for 15 sec) and annealing (various temperatures for 15 sec), extension (72°C for 60 sec). The primer sequences and annealing temperatures are provided in **Table S3**. Relative gene expression was determined using the Pfaffl method to account for differential primer efficiencies (Pfaffl 2001), using the geometric mean of the Cq values for beta-2-microglobulin (*B2m*) and 18s ribosomal RNA (*Rn18s*) for mouse gene normalization and of ribosomal protein L27 (*RPL27*) and *B2M* for human gene normalization. The Cq value from naïve, pre-adipocyte cultures was used as the reference point. Data are reported as "Relative Expression."

Cell Death

3T3-L1 cells or human preadipocytes were plated in 96 well, black-sided plates at 10,000 cells per well in 0.2 ml maintenance medium at initiation of the experiment. Dosing is outlined in **Table 1**. Cells death was measured by treating differentiated cells will MitoOrange Dye

according to manufacturer's protocol (Abcam, Cambridge, MA). Measurement of fluorescence intensity (λex= 485 nm, λem= 530 nm) was performed using a Synergy2 plate reader. The fluorescence in experimental wells was normalized by subtracting the fluorescence measured in naïve pre-adipocyte cultures and reported as "RFU."

Fatty Acid Uptake

3T3-L1 cells or human preadipocytes were plated in 96 well, black-sided plates at 10,000 cells per well in 0.2 ml maintenance medium at initiation of the experiment. Dosing is outlined in **Table 1**. Fatty acid uptake was measured by treating differentiated cells with 100 µL of Fatty Acid Dye Loading Solution (Sigma-Aldrich, MAK156). Following a 1 hr incubation, measurement of fluorescence intensity (λex= 485nm, λem= 530nm) was performed using a Synergy2 plate reader. The fluorescence in experimental wells was normalized by subtracting the fluorescence in differentiated, negative control wells and reported as "RFU."

Mitochondrial Biogenesis

3T3-L1 cells or human preadipocytes were plated in 24 well plates at 50,000 cells per well in 0.5 ml maintenance medium at initiation of the experiment. Dosing is outlined in **Table 1**. Mitochondrial biogenesis was measured in differentiated cells using the MitoBiogenesis In-Cell Elisa Colorimetric Kit, following the manufacturer's protocol (Abcam). The expression of two mitochondrial proteins (COX1 and SDH) were measured simultaneously and normalized to the total protein content via JANUS staining. Absorbance (OD 600nm for COX1, OD 405nm for SDH, and OD 595nm for JANUS) was measured using a BioTek Synergy2 plate reader. The absorbance ratios of COX/SDH in experimental wells were divided by the ratios in naïve pre-adipocyte cultures and reported as "Relative Mitochondrial Protein Expression."

Oxygen Consumption

3T3-L1 cells or human preadipocytes were plated in Agilent Seahorse plates at 50,000 cells per well in 0.5 ml maintenance medium at initiation of the experiment. Dosing is outlined in **Table 1**. Prior to all assays, cell media was changed to Seahorse XF Assay Medium without glucose (1mM sodium pyruvate, 1mM GlutaMax, pH 7.4) and incubated at 37°C in a non-CO_2 incubator for 30 min. To measure mitochondrial respiration, the Agilent Seahorse XF96 Cell Mito Stress Test Analyzer (available at BUMC Analytical Instrumentation Core) was used, following the manufacturer's standard protocol. The compounds and their concentrations used to determine oxygen consumption rate (OCR) included 1) 0.5 μM oligomycin, 1.0 μM carbonyl cyanide-p-trifluoromethoxyphenylhydrazone (FCCP) and 2 μM rotenone for 3T3-L1s; and 2) 5 μM oligomycin, 2.5 μM FCCP, and 10 μM rotenone for the primary human adipocytes. Non-mitochondrial respiration was determined from the minimum rate measurement after injection of rotenone. Basal respiration was determined by subtracting non-mitochondrial respiration from the last rate measurement before the injection of ologomycin. Maximum respiration was determined by subtracting non-mitochondrial respiration from the maximum rate measurement after the injection of FCCP. Spare capacity was determined by subtracting the basal respiration from the maximum respiration.

Statistical Analyses

All statistical analyses were performed in R (v 3.4.3) and Prism 7 (GraphPad Software, Inc., La Jolla, CA). Data are presented as means ± standard error (SE). For 3T3-L1 experiments the biological replicates correspond to independently plated experiments. For human primary preadipocyte experiments the biological replicates correspond to distinct individuals' preadipocytes (3 individuals in all). The Nile Red data and the qPCR data were not normally distributed; therefore, the data were log transformed before statistical analyses. One-factor

ANOVAs (Dunnett's) were performed to analyze the qPCR and phenotypic data and determine differences from vehicle-treated cells. Sequencing data from 3'DGE have been deposited into GEO (Accession: GSE124564).

Results

Classification of novel taxonomic subgroups of PPARγ ligands/modifiers

Potential adipogens (chemicals that change the differentiation and/or function of adipocytes) were identified by review of the literature and based on reports of PPARγ agonism or modulation of adipocyte differentiation (**Table S1)**. Our classification groups were labeled as "Yes", "No", or "Suspected", based on the chemical's potential ability to act as a ligand of or modify PPARγ (i.e., to alter its post translational modifications) as noted in the "PPARγ Ligand or Modifier" column in **Table S1**.

The classic mouse pre-adipocyte model, 3T3-L1 cells, was differentiated and treated with vehicle (DMSO) or with each of the 76 test chemicals (concentrations are reported in **Table S1**). In order to maximize the number of chemicals that could be characterized, each chemical was tested at a single, maximal, non-toxic dose. We also limited the maximum concentrations to 20 μM because concentrations above this would not be reached in humans and because most (although not all) chemicals are not toxic at or below 20 μM. Lipid accumulation was determined after 10 days. Effects on lipid accumulation spanned significant down-regulation to significant up-regulation (**Figure 1**). Lipid accumulation was highly correlated with expression of adipocyte specific genes (e.g. *Cidec* (Danesch et al. 1992), **Figure S2**); therefore, we consider it a biomarker of adipocyte differentiation in this system. Of the 27 chemicals that significantly increased lipid accumulation, 18 were known PPARγ ligands/modifiers and 9 were suspected

PPARγ ligands/modifiers. Mono(2-ethylhexyl) phthalate (MEHP), SR1664, and 15-deoxy-$\Delta^{12,14}$-prostaglandin J2 (15dPGJ2) are PPARγ agonists that were expected to increase adipocyte differentiation, but did not. LG268 and TBT are RXR agonists that were also expected to significantly increase adipocyte differentiation, but did not. The 3 chemicals that significantly down-regulated lipid accumulation are all known to interact with the retinoic acid receptor. T007 is a PPARγ antagonist that was expected to decrease adipocyte differentiation, but did not. Some of the suspected PPARγ ligands did not significantly enhance lipid accumulation.

Following the analysis of lipid accumulation, RNA was isolated from the cells, and the transcriptome was characterized by RNA-Seq. The transcriptome data then were used to develop a classification model to identify PPARγ ligands/modifiers. More specifically, the *training set* of 59 chemicals with "Yes"/"No" labels was used to build the classifier, which was then applied to the prediction of the *test set* of 17 "Suspected" chemicals. When predicting PPARγ ligand/modifier status ("Yes" *vs.* "No"), the mean AUC, precision, sensitivity, specificity, F1-score, and balanced accuracy from repeated 10-fold cross validation (over the training set) of the random forest with bag merging procedure was 0.89, 0.90, 0.80, 0.85, 0.85, and 0.82, respectively (**Figure 2A**). We observed the most drastic improvement of measured balanced accuracy, precision, and specificity by the bag merging procedure compared to other assessed strategies (**Figure S3**). The first two metrics in particular (AUC and precision) reflect expectation of relatively few false positive results compared to the other strategies. In the final model, the voting threshold that produced the highest F1-score was 0.53. When we applied the classifier to the test set of the 17 chemicals of unknown interaction with PPARγ, 13 had random forest votes greater than this value (**Table 2**). Of these 13 compounds, four had votes > 0.88. These chemicals included quinoxyfen, tonalide, allethrin, and fenthion. These compounds were

predicted as PPARγ ligands/modifiers with high confidence and were selected for further functional analyses. Of the 1,215 genes that past ANOVA filtering and were included in the random forest models, ribosomal protein L13 (*Rpl13*) and cell death Inducing DFFA Like Effector C (*Cidec*) had the highest measured Gini Importance (**Figure 2B**) with *Rpl13* mostly down-regulated and *Cidec* mostly up-regulated by known PPARγ ligands/modifiers (**Figure S4**). Gene specific ANOVA filtering results and importance estimates, as well as out-of-bag voting estimates for each compound in the training set can be found in **Table S4**.

Adipogen Taxonomy Discovery

The taxonomy derived by the K2 Taxonomer procedure recapitulated many known characteristics shared by PPARγ ligands/modifiers included in this study (**Figure 3**). For example, three terminal subgroups were labelled in **Figure 3** based on their shared characteristics. These include: flame retardants (tetrabromobisphenol A (TBBPA) and triphenyl phosphate (TPhP)), phthalates (MBUP, MEHP, MBZP, and BBZP), and RXR agonists (TBT and LG268). Interestingly, we observed two subgroups containing all of the four thiazolidinediones, with rosiglitazone (Rosig) segregating with the non-thiazolidinedione S26948 and pioglitazone, MCC 555, and troglitazone segregating together. Comprehensive functional annotation of the gene signatures and enriched pathways for comparisons between sub-groups at each split can be found in **Table S5**.

All of these terminal subgroups fell within a larger module containing 26 chemicals, highlighted by expression patterns consistent with increased adipogenic activity including up-regulation of genes significantly enriched in pathways involved in adipogenesis and lipid metabolism (Soukas et al. 2001). In addition, these chemicals also demonstrated consistent down-regulation of extracellular component genes. This effect was strongest in cells exposed to

thiazolidinediones and flame retardants, two classes of chemicals well-described to be strong PPARγ agonists (Berger et al. 1996; Fang et al. 2015a; Riu et al. 2011). The subgroup of thiazolidinediones, including S26948, was characterized by up-regulation of genes involved in beta-oxidation, the process by which fatty acids are metabolized.

The gene expression profiles of the remaining 17 chemicals, including naïve pre-adipocytes, demonstrate markedly less up-regulation of genes regulated by PPARγ. Of these 17 perturbations, a subgroup of 8 chemicals (BADGE, PrPar, 15dPGJ2, SR1664, METBP, DINP, BuPA, and Fenth) includes the reference vehicle signature. Compared to the next closest subgroup, expression profiles of these compounds was characterized by up-regulation of adipogenesis-related pathways indicative of modest PPARγ agonism. Additionally, a subgroup comprised of 9CRA, DBT, LG754, and ATRA exposures and naïve pre-adipocyte signatures was characterized by down-regulation of genes involved in adipogenesis and lipid metabolism, indicating repression of PPARγ activity. Interestingly, both protectin D1 (Prote) and resolvin E1 (Resol) clustered closely in a subgroup with the CDK inhibitor, roscovitine (Rosco), which is known to induce insulin sensitivity and brite adipogenesis (Wang et al. 2016).

In summary, our top-down taxonomy discovery approach elucidated subgroups of PPARγ ligands/modifiers, characterized by differential transcriptomic activity at each split. Annotation of these transcriptomic signatures revealed clear differences in the set and magnitude of perturbations to known adipocyte biological processes by subgroups of chemicals. Membership of these subgroups confirmed many expectations, such as subgroups comprised solely of phthalates, thiazolidinediones, or flame retardants

Relationship between taxonomic subgroups and the human adipose transcriptome

Given that our taxonomic clustering was based on adipogen exposures in a mouse model, we sought to establish its relevance to the relationship between human adipose tissue function and markers of cardio-metabolic health. To this end, we projected the gene signatures derived as either up- or down-regulated gene sets in specific taxonomic subgroups onto a publicly available clinical data set of gene expression profiles from subcutaneous adipose tissue of 770 male subjects and assessed the relationship of these projections to a set of 12 clinical measurements (Civelek et al. 2017). **Figure 4A-B** shows the partial correlation between plasma adiponectin and projection of gene sets, either up- or down-regulated in specific subgroups (further details are provided in **Table S6**). **Figure 4C** shows these relationships for the remaining measurements which demonstrated a statistically significant partial correlation for at least one projection, FDR Q-value < 0.10. For positive associations, i.e. in the same direction, the up-regulated gene sets have positive partial correlation measurements, while down-regulated gene sets have negative partial correlation measurements. The opposite is true for negative associations.

We observed concordant results for putative markers of metabolic health, plasma adiponectin and fat free mass %, which were positively associated with projection of gene signatures from two terminal subgroups which include all TZD and non-TZD type 2 diabetic drugs, Trogl, MCC555, Piogl, Rosig, and S26948, as well as a terminal subgroup which includes Rosco, Resol, and Protec. Similary, we observed concordant results for putative markers of metabolic dysfunction, interleukin-1 receptor antagonist and fasting plasma insulin, which included a primary subgroup comprised of terminal subgroups characterized by weak PPARγ agonism, PPARγ modification, or PPARγ activity repression.

Taken together, these results confirm the ability of our mouse-based, in vitro-derived signatures of capturing salient functional aspects of healthy and unhealthy metabolic functions in human subjects.

Investigation of the white and brite adipocyte taxonomy

We aimed to better assess how the distinction between gene expression patterns translated into functional differences in the induced adipocytes. Therefore, we selected chemicals from representative groups related of PPARγ ligands/modifiers for genotypic and phenotypic characterization. We compared a strong PPARγ therapeutic agonist that also modifies PPARγ phosphorylation (Rosig), a chemical that modifies only PPARγ phosphorylation (Rosco), a weak PPARγ agonist and endogenous molecule (15dPGJ2) and two known environmental PPARγ ligands (TBBPA and TPhP). 3T3-L1 cells were differentiated and treated with vehicle (DMSO), Rosig (positive control, 20 μM), Rosco (2 μM), 15dPGJ2 (1 μM), TBBPA (20 μM) and TPhP (10 μM). Gene expression and phenotype were determined after 10 days. Analysis of mitochondrial membrane potential confirmed that the concentrations used were not toxic (**Figure S5A**), while only Rosig significantly increased cell number (**Figure S5B**).

First, we determined if changes in gene expression correlated with expression of genes previously shown to be associated with white and brite adipocytes (Qiang et al. 2012). As expected, all of the PPARγ agonists (Rosig, 15dPGJ2, TBBPA, TPhP) significantly increased *Pparg* expression, while Rosco did not (**Figure 5A**). Similarly, the PPARγ agonists induced expression of adipocyte genes common to all adipocytes (*Plin*, *Fabp4*, *Cidec*), while roscovitine did not (**Figure 5B**). In contrast, only the chemicals known to prevent phosphorylation of PPARγ at Ser273 (i.e., Rosig and Rosco) induced expression of *Pgc1a* (**Figure 5A**) and induced expression of brite adipocyte genes (*Cidea*, *Elovl3*) (**Figure 5C**). Rosig, Rosco, and 15dPGJ2

induced the expression of *Adipoq* (**Figure 5C**). In order for brite adipocytes to catabolize fatty acids and expend excess energy, they must up-regulate expression of β-oxidation genes and mitochondrial biogenesis. In line with their browning capacity, Rosig and Rosco up-regulated expression of *Ppara* and the mitochondrial marker gene *Acaa2* (**Figure 5D**). Furthermore, only Rosig and Rosco strongly up-regulated *Ucp1*, the protein product of which dissociates the H^+ gradient the mitochondrial electron transport chain creates from ATP synthesis (**Figure 5D**).

Next, we determined if changes in gene expression correlated with changes in adipocyte function. 3T3-L1 cells were differentiated and treated as described for the mRNA expression analyses. Fatty acid uptake by adipocytes is necessary for lipid droplet formation and for removal of free fatty acids from circulation. Compared to vehicle-treated cells, all of the adipogens significantly induced fatty acid uptake (**Figure 6**). In order to increase the utilization of fatty acids, mitochondrial number and/or function must increase. Only Rosig and Rosco significantly induced mitochondrial biogenesis, while 15dPGJ2 and the environmental PPARγ agonists had no effect (**Figure 7**). Rosig modestly and 15dPGJ2 significantly increased cellular respiration (**Figure 8**, **Figure S6**). Rosco, TBBPA and TPhP did not increase cellular respiration.

Overall, Rosig and Rosco, therapeutic PPARγ ligand and PPARγ modifier, respectively, were most efficacious at inducing gene expression and metabolic phenotypes related to up-regulation of mitochondrial processes and energy expenditure. In comparison, environmental PPARγ ligands (TBBPA and TPhP) were not able to induce the gene and phenotypic markers of brite adipocytes.

Identification of novel adipogens that favor white adipogenesis

Quinoxyfen (Quino) and tonalide (Tonal) were two of the environmental chemicals that received the highest PPARγ ligand/modifier vote and segregated distinctly from the therapeutic

ligands (**Table 2**). Thus, we tested the hypothesis that Quino and Tonal are adipogens that do not induce gene expression or metabolic phenotypes indicative of high energy expenditure or brite adipogenesis. 3T3-L1 cells were differentiated and treated with vehicle (DMSO), rosiglitazone (positive control, 20 μM), Quino (10 μM), or Tonal (4 μM). These concentrations were determined to be non-toxic (**Figure S7A**). .In 3T3-L1 cells, Quino and Tonal significantly induced lipid accumulation (**Figure 9A**), without increasing cell number (**Figure S7B**). They significantly increased expression of the white adipocyte marker gene, *Cidec.* However, Quino failed to significantly increase expression of *Cidea*, the brite adipocyte marker gene, while Tonal significantly suppressed expression of *Cidea* (**Figure 9B**). Accordingly, Quino and Tonal increased fatty acid uptake (**Figure 9C**) but not mitochondrial biogenesis (**Figure 9D**). Quino modestly, but not significantly, increased maximal cellular respiration; Tonal had no effect on cellular respiration (**Figure 8**).

Last, we investigated whether results in our mouse model, 3T3-L1 cells, could be recapitulated in a human model. Primary, human subcutaneous preadipocytes were differentiated and treated with vehicle (DMSO), rosiglitazone (positive control, 4 μM), Quino (4 μM), or Tonal (4 μM). Quino and Tonal significantly induced lipid accumulation (**Figure 10A**). Tonal, but not Quino, increased cell number (**Figure S7C**). Both Quino and Tonal failed to induce *CIDEA* expression expression (**Figure 10B**). In contrast to 3T3-L1 cells, Quino and Tonal did not increase fatty acid uptake over that induced by the hormonal cocktail in the differentiated primary human adipocytes (**Figure 10C**). Quino and Tonal also reduced mitochondrial biogenesis (**Figure 10D**).

In summary, the combination of random forest classification voting and gene expression clustering identified two environmental contaminants likely to favor the induction of white

adipocytes. Hypothesis testing carried out with functional analyses confirmed that Quino and Tonal induce white, but not brite, adipogenesis in both mouse and human preadipocyte models. Importantly, we demonstrate that hypothesis testing can be conducted with readily available cells lines and analytical reagents.

Discussion

The chemical environment has changed dramatically in the past 40 years, and an epidemic increase in the prevalence of obesity has occurred over the same time period. Yet, it is still unclear how chemical exposures may be contributing to adverse metabolic health effects. New tools are needed not just to identify potential adipogens, but to provide information on the type of adipocyte that is formed. Here, we have both developed a new analytical framework for adipogen identification and characterization and tested its utility in hypothesis generation. We show that adipogens segregate based on distinct patterns of gene expression, which we used to identify two environmental contaminants for hypothesis testing. Our results support the conclusion that quinoxyfen and tonalide have a limited capacity to induce the health-promoting effects of mitochondrial biogenesis and brite adipocyte differentiation.

Adipogen taxonomy identifies environmental chemicals that favor white adipogenesis

Potential adipogens (chemicals that change the differentiation and/or function of adipocytes) were identified by review of the literature and based on reports of PPARγ agonism or modulation of adipocyte differentiation, as well as through querying ToxCast data. Not all of the chemicals identified as PPARγ ligands/modifiers induced significant lipid accumulation. We hypothesize that this likely resulted from the fact that we did not apply any chemical above 20 μM (with the exception of fenthion). Concentrations in the 100 μM range have been used in

previous studies (e.g. DOSS (Temkin et al. 2016); parabens (Hu et al. 2013); phthalates (Hurst and Waxman 2003)). The RXR agonists LG268 and TBT also were expected to significantly increase adipocyte differentiation, but did not. We have previously shown that TBT induces adipogenesis with greater efficacy in OP9 cells rather than 3T3-L1 cell (Kassotis et al. 2017).

We identified four compounds as high-confidence PPARγ ligands/modifiers: quinoxyfen, tonalide, allethrin, and fenthion. In the final model used for these predictions, biologically informative genes emerge as important for predicting PPARγ ligand/modification status, specifically the down-regulation of *Rpl13* and the up-regulation of *Cidec*. *Rpl13* is involved in ribosomal machinery is down-regulated during human adipogensis (Marcon et al. 2017). *Cidec* is a lipid droplet structural gene, the expression of which is positively correlated with adipocyte lipid droplet size, insulin levels, and glycerol release (Ito et al. 2010). Of these four compounds, quinoxyfen and tonalide are of particular public health concern. Quinoxyfen is among a panel of pesticides with different chemical structures and modes of action (i.e., zoxamide, spirodiclofen, fludioxonil, tebupirimfos, forchlorfenuron, flusilazole, acetamaprid, and pymetrozine) that induce adipogenesis and adipogenic gene expression in 3T3-L1 cells (Janesick et al. 2016). Quinoxyfen is a fungicide widely used to prevent the growth of powdery mildew on grapes (Duncan et al. 2018). We chose to test tonalide because it was reported to strongly increase adipogenesis in 3T3-L1 cells, although it was concluded that this response was not due to direct PPARγ activation (Pereira-Fernandes et al. 2013). Our results differ in this regard. Tonalide bioaccumulates in adipose tissue of many organisms including humans, and exposure is widespread because of its common use in cosmetics and cleaning agents (Kannan et al. 2005). Combined, tonalide and galaxolide constitute 95% of the polycyclic musks used in the EU market and 90% of that of the US market (HERA 2004).

Our results support the conclusion that quinoxyfen and tonalide are adipogenic chemicals, likely to be acting through PPARγ. In clustering analysis, quinoxyfen and tonalide were among the largest subgroup of eight potential strong PPARγ agonists. Notably, this cluster includes both synthetic/therapeutic (nTZDpa, tesaglitazar, telmisartan) and environmental compounds (tributyl phosphate and triphenyltin) and is characterized by general up-regulation of pathways of adipogenic activity. However, quinoxyfen and tonalide generate adipocytes that are phenotypically distinct from adipocytes induced by therapeutics such as rosiglitazone. That environmental PPARγ ligands can induce a distinct adipocyte phenotype has been shown previously for TBT (Kim et al. 2018; Regnier et al. 2015; Shoucri et al. 2018) and TPhP (Kim et al. 2020).

We tested the effect of quinoxyfen and tonalide on human subcutaneous preadipocyte differentiation. There is a strong association between abdominal adiposity and metabolic syndrome (Cornier et al. 2008). Classically, visceral adipose tissue has been thought to be the driver of metabolic dysfunction; however, there is an alternative explanation that visceral adiposity results secondarily from the dysfunction of subcutaneous adipose tissue in the upper body (Jensen 2008; Lee et al. 2017). While humans have greater "browning" potential in their visceral adipose tissue than mice (Zuriaga et al. 2017), subcutaneous adipose represents 85% of all body fat (Frayn and Karpe 2014) and thus has a large overall capacity for generating brite adipocytes. Additionally, lack of browning capacity of human subcutaneous adipocytes is associated with insulin resistance (Yang et al. 2003). As hypothesized based on the taxonomical analysis, quinoxyfen and tonalide induced white adipocyte functions such as increased lipid accumulation, but in contrast to rosiglitazone, did not induce mitochondrial biogenesis, energy expenditure or brite adipocyte gene expression.

We hypothesize that the differences in adipocyte phenotype that are induced by environmental PPARγ ligands (e.g. TBBPA, TPhP, quinoxyfen, tonalide) result from the conformation that PPARγ assumes when liganded with these chemicals rather than with therapeutic agents. These differences in conformation not only determine the efficacy to which PPARγ is activated but also the transcriptional repertoire (Chrisman et al. 2018). Consistent with this hypothesis, we observed multiple terminal subgroups of PPARγ ligands/modifiers of shared properties, specifically TZDs and non-TZD type 2 diabetic drugs, phthalates, and flame retardants. Furthermore, subgroups containing therapeutics share gene expression patterns in human adipose tissue in accordance with positive markers of metabolic health, specifically plasma adiponectin and fat free mass (%), suggesting that these gene expression are related to metabolic health in humans.

Access to post-translational modification sites and coregulator binding surfaces depends upon the structure that PPARγ assumes. The white adipogenic, brite/brown adipogenic and insulin sensitizing activities of PPARγ are regulated separately through differential co-regulator recruitment (Villanueva et al. 2013) and post-translational modifications (Choi et al. 2010; Choi et al. 2011), with ligands having distinct abilities to activate each of PPARγ's functions. Suites of genes have been shown to be specifically regulated by the acetylation status of PPARγ (SirT1-mediated) (Qiang et al. 2012), by the phosphorylation status of PPARγ (ERK/MEK/CDK5-mediated) (Choi et al. 2010; Wang et al. 2016) and/or by the recruitment of Prdm16 to PPARγ (Seale et al. 2007). Future work will investigate the connections between the phosphorylation status of PPARγ liganded with environmental PPARγ ligands such as quinoxyfen and tonalide, the recruitment and release of coregulators, and the ability of PPARγ to recruit transcriptional

machinery to specific DNA-binding sites. It will be important to determine the metabolic effects of chemicals like quinoxyfen and tonalide *in vivo.*

Analytical approaches for adipogen characterization

In this study, we performed a high-throughput, cost-effective transcriptomic screening to profile adipocytes formed from 3T3-L1 preadipocytes exposed to a panel of compounds of known and unknown adipogenic impact. Common to toxicogenomic projects, this panel-based study design allows for characterization of the extent to which each chemical modifies differentiation (in this case, adipogenesis as related to the change in lipid accumulation). It also supports the exploration of how subsets of chemicals influence multiple biological processes that determine the functional status of a cell (in this case, processes that determine white *vs.* brite adipogenesis). Exploration of these biological processes allows for the prediction of the phenotypic impact of previously unclassified compounds, as well as for the characterization of the heterogeneity of the cellular activity of compounds with similar known phenotypic impact. Here we have performed both types of analyses: first through the implementation and application of random forest classification models to identify potential PPARγ ligands/modifers, and second via the recursive clustering of the data to identify and characterize taxonomic subgroup of known and predicted PPARγ ligands/modifiers.

For both analyses, we introduced amendments to commonly used machine learning procedures, to improve accuracy and resolution of the acquired result. For the classification task, we amended the random forest algorithm to tailor it to study designs typically adopted in toxicogenomic projects (see Methods). With the addition of an extra step to average the expression across replicates of the bootstrapped samples, we observe consistently higher performance across conventional metrics than with the standard algorithm. For the clustering

task, we employ a procedure where we recursively divide sets of chemicals into two subgroups and assess the robustness of each division, as well as annotate transcriptional drivers of each division. As a result, we are not limited to interpreting the clustering results as mutually exclusive groups, but rather as a taxonomy of subgroups where sets of compounds share some transcriptional impact and differ in others, as is expected given the dynamic nature of the modifications by which compounds directly and indirectly affect PPARγ activity.

Future work will generalize random forest method to incorporate more complex study designs. To this end, the classification approach adopted in this project is being developed as a random forest software tool soon to be made available as an R package, allowing for the interchanging independent functions at different steps of the algorithm. The strength and utility of this approach extends beyond toxicogenomic studies, and can be used in a variety of applications of high-throughput screening, including drug discovery, such as the Connectivity Map (CMAP) (Subramanian et al. 2017), and longitudinal molecular epidemiology studies, such as the Framingham Heart Study (Mahmood et al. 2014).

Adipogen portal

Given the breadth of results generated by this analysis, our description here is far from exhaustive. As such, we have created an interactive website (https://montilab.bu.edu/adipogenome/) to support the interactive exploration of these results at both the gene and pathway-level. A screenshot and description of how to navigate this web portal is given in **Figure S8**. The portal is built around a point-and-click dendrogram of the clustering results as in **Figure 3**. Selecting a node of this dendrogram will populate the rest of the portal with the chemical lists, differential analysis, and pathway level hyper-enrichment results for each subgroup defined by a split. For instance, selecting node “H” will show the

chemicals in each subgroup to the right (Group 1 = Honokiol, T007907; Group 2 = Prote, Resol, and Rosco), as well as the differential gene signature for each group below. Selecting *Cidec*, the top gene in the Group 2 signature, displays hyper-enrichment results for gene sets which include *Cidec* and have a nominal p-value < 0.50. The hyper-enrichment results for all genes can be found below this table. Finally, selecting a gene set name will display the gene set members at the bottom frame of the portal, with gene hits in bold. All tables are query-able and downloadable.

Conclusions

Emerging data implicate contributions of environmental metabolism-disrupting chemicals to perturbations of pathways related to metabolic disease pathogenesis, such as disruptions in insulin signaling and mitochondrial activity. There is still a gap in identifying and examining how environmental chemicals can act as obesity-inducing and metabolism-disrupting chemicals. Our implementation of novel strategies for classification and taxonomy development can help identify environmental chemicals that are acting on PPARγ. Further, our approach provides a basis from which to investigate effects of adipogens on not just the generation of adipocytes, but potentially pathological changes in their function. To this end, we have shown how two environmental contaminants, quinoxyfen and tonalide, are inducers of white adipogenesis.

References:

.

Auerbach S, Filer D, Reif D, Walker V, Holloway AC, Schlezinger J, et al. 2016. Prioritizing environmental chemicals for obesity and diabetes outcomes research: A screening approach using toxcast high-throughput data. Environ Health Perspect 124:1141-1154.

Banks AS, McAllister FE, Camporez JP, Zushin PJ, Jurczak MJ, Laznik-Bogoslavski D, et al. 2015. An erk/cdk5 axis controls the diabetogenic actions of ppargamma. Nature 517:391-395.

Berger J, Bailey P, Biswas C, Cullinan CA, Doebber TW, Hayes NS, et al. 1996. Thiazolidinediones produce a conformational change in peroxisomal proliferator-activated receptor-gamma: Binding and activation correlate with antidiabetic actions in db/db mice. Endocrinology 137:4189-4195.

Burgermeister E, Schnoebelen A, Flament A, Benz J, Stihle M, Gsell B, et al. 2006. A novel partial agonist of peroxisome proliferator-activated receptor-gamma (ppargamma) recruits ppargamma-coactivator-1alpha, prevents triglyceride accumulation, and potentiates insulin signaling in vitro. Mol Endocrinol 20:809-830.

Cano-Sancho G, Smith A, La Merrill MA. 2017. Triphenyl phosphate enhances adipogenic differentiation, glucose uptake and lipolysis via endocrine and noradrenergic mechanisms. Toxicol In Vitro 40:280-288.

Choi JH, Banks AS, Estall JL, Kajimura S, Bostrom P, Laznik D, et al. 2010. Anti-diabetic drugs inhibit obesity-linked phosphorylation of ppargamma by cdk5. Nature 466:451-456.

Choi JH, Banks AS, Kamenecka TM, Busby SA, Chalmers MJ, Kumar N, et al. 2011. Antidiabetic actions of a non-agonist ppargamma ligand blocking cdk5-mediated phosphorylation. Nature 477:477-481.

Chrisman IM, Nemetchek MD, de Vera IMS, Shang J, Heidari Z, Long Y, et al. 2018. Defining a conformational ensemble that directs activation of ppargamma. Nat Commun 9:1794.

Civelek M, Wu Y, Pan C, Raulerson CK, Ko A, He A, et al. 2017. Genetic regulation of adipose gene expression and cardio-metabolic traits. Am J Hum Genet 100:428-443.

Claussnitzer M, Dankel SN, Kim KH, Quon G, Meuleman W, Haugen C, et al. 2015. Fto obesity variant circuitry and adipocyte browning in humans. The New England journal of medicine 373:895-907.

Cornier MA, Dabelea D, Hernandez TL, Lindstrom RC, Steig AJ, Stob NR, et al. 2008. The metabolic syndrome. Endocr Rev 29:777-822.

Danesch U, Hoeck W, Ringold GM. 1992. Cloning and transcriptional regulation of a novel adipocyte-specific gene, fsp27. Caat-enhancer-binding protein (c/ebp) and c/ebp-like proteins interact with sequences required for differentiation-dependent expression. J Biol Chem 267:7185-7193.

Duncan H, Abad-Somovilla A, Abad-Fuentes A, Agullo C, Mercader JV. 2018. Immunochemical rapid determination of quinoxyfen, a priority hazardous pollutant. Chemosphere 211:302-307.

Fang M, Webster TF, Ferguson PL, Stapleton HM. 2015a. Characterizing the peroxisome proliferator-activated receptor (ppargamma) ligand binding potential of several major flame retardants, their metabolites, and chemical mixtures in house dust. Environ Health Perspect 123:166-172.

Fang M, Webster TF, Stapleton HM. 2015b. Effect-directed analysis of human peroxisome proliferator-activated nuclear receptors (ppargamma1) ligands in indoor dust. Environ Sci Technol 49:10065-10073.

Farmer SR. 2006. Transcriptional control of adipocyte formation. Cell metabolism 4:263-273.

Feige JN, Gelman L, Rossi D, Zoete V, Metivier R, Tudor C, et al. 2007. The endocrine disruptor monoethyl-hexyl-phthalate is a selective peroxisome proliferator-activated receptor gamma modulator that promotes adipogenesis. J Biol Chem 282:19152-19166.

Frayn KN, Karpe F. 2014. Regulation of human subcutaneous adipose tissue blood flow. International journal of obesity (2005) 38:1019-1026.

GBD. 2017. Health effects of overweight and obesity in 195 countries over 25 years. The New England journal of medicine 377:13-27.

Gumbilai V, Ebihara K, Aizawa-Abe M, Ebihara C, Zhao M, Yamamoto Y, et al. 2016. Fat mass reduction with adipocyte hypertrophy and insulin resistance in heterozygous ppargamma mutant rats. Diabetes 65:2954-2965.

Hanzelmann S, Castelo R, Guinney J. 2013. Gsva: Gene set variation analysis for microarray and rna-seq data. BMC Bioinformatics 14:7.

He W, Barak Y, Hevener A, Olson P, Liao D, Le J, et al. 2003. Adipose-specific peroxisome proliferator-activated receptor gamma knockout causes insulin resistance in fat and liver but not in muscle. Proc Natl Acad Sci U S A 100:15712-15717.

Heindel JJ, Blumberg B, Cave M, Machtinger R, Mantovani A, Mendez MA, et al. 2017. Metabolism disrupting chemicals and metabolic disorders. Reproductive toxicology (Elmsford, NY 68:3-33.

HERA. 2004. Human & environmental risk assessment on ingredients of household cleaning products: Polycyclic musks. Available: https://www.heraproject.com/files/29-E-04_pcm_HHCB_AHTN_HERA_Environmenta_DISCLed26.pdf [accessed Dec. 27 2018].

Hiromori Y, Ido A, Aoki A, Kimura T, Nagase H, Nakanishi T. 2016. Ligand activity of group 15 compounds possessing triphenyl substituent for the rxr and ppargamma nuclear receptors. Biol Pharm Bull 39:1596-1603.

Hu P, Chen X, Whitener RJ, Boder ET, Jones JO, Porollo A, et al. 2013. Effects of parabens on adipocyte differentiation. Toxicol Sci 131:56-70.

Hurst CH, Waxman DJ. 2003. Activation of ppara and pparg by environmental phthalate monoesters. Toxicol Appl Pharmacol.

Ito M, Nagasawa M, Hara T, Ide T, Murakami K. 2010. Differential roles of cidea and cidec in insulin-induced anti-apoptosis and lipid droplet formation in human adipocytes. Journal of lipid research 51:1676-1684.

Janesick AS, Dimastrogiovanni G, Vanek L, Boulos C, Chamorro-Garcia R, Tang W, et al. 2016. On the utility of toxcast and toxpi as methods for identifying new obesogens. Environ Health Perspect 124:1214-1226.

Jensen MD. 2008. Role of body fat distribution and the metabolic complications of obesity. J Clin Endocrinol Metab 93:S57-63.

Jiang Y, Berry DC, Tang W, Graff JM. 2014. Independent stem cell lineages regulate adipose organogenesis and adipose homeostasis. Cell Rep 9:1007-1022.

Kannan K, Reiner JL, Yun SH, Perrotta EE, Tao L, Johnson-Restrepo B, et al. 2005. Polycyclic musk compounds in higher trophic level aquatic organisms and humans from the united states. Chemosphere 61:693-700.

Kassotis CD, Masse L, Kim S, Schlezinger JJ, Webster TF, Stapleton HM. 2017. Characterization of adipogenic chemicals in three different cell culture systems: Implications for reproducibility based on cell source and handling. Sci Rep 7:42104.

Kavlock R, Chandler K, Houck K, Hunter S, Judson R, Kleinstreuer N, et al. 2012. Update on epa's toxcast program: Providing high throughput decision support tools for chemical risk management. Chem Res Toxicol 25:1287-1302.

Kim S, Li A, Monti S, Schlezinger JJ. 2018. Tributyltin induces a transcriptional response without a brite adipocyte signature in adipocyte models. Arch Toxicol 92:2859-2874.

Kim S, Rabhi N, Blum B, Hekman R, Wynne K, Emili A, et al. 2020. Triphenyl phosphate is a selective pparγ modulator that does not induce brite adipogenesis in vitro and in vivo. . Arch Toxicol Submitted for publication:BIORXIV 626390.

Lee JJ, Pedley A, Therkelsen KE, Hoffmann U, Massaro JM, Levy D, et al. 2017. Upper body subcutaneous fat is associated with cardiometabolic risk factors. Am J Med 130:958-966 e951.

Lee MJ, Fried SK. 2014. Optimal protocol for the differentiation and metabolic analysis of human adipose stromal cells. Methods Enzymol 538:49-65.

Mahmood SS, Levy D, Vasan RS, Wang TJ. 2014. The framingham heart study and the epidemiology of cardiovascular disease: A historical perspective. Lancet 383:999-1008.

Marcon BH, Holetz FB, Eastman G, Origa-Alves AC, Amoros MA, de Aguiar AM, et al. 2017. Downregulation of the protein synthesis machinery is a major regulatory event during early adipogenic differentiation of human adipose-derived stromal cells. Stem Cell Res 25:191-201.

O'Donnell PE, Ye XZ, DeChellis MA, Davis VM, Duan SZ, Mortensen RM, et al. 2016. Lipodystrophy, diabetes and normal serum insulin in ppargamma-deficient neonatal mice. PloS one 11:e0160636.

Ohno H, Shinoda K, Spiegelman BM, Kajimura S. 2012. Ppargamma agonists induce a white-to-brown fat conversion through stabilization of prdm16 protein. Cell metabolism 15:395-404.

Park YW, Zhu S, Palaniappan L, Heshka S, Carnethon MR, Heymsfield SB. 2003. The metabolic syndrome: Prevalence and associated risk factor findings in the us population from the third national health and nutrition examination survey, 1988-1994. Arch Intern Med 163:427-436.

Pereira-Fernandes A, Demaegdt H, Vandermeiren K, Hectors TL, Jorens PG, Blust R, et al. 2013. Evaluation of a screening system for obesogenic compounds: Screening of endocrine disrupting compounds and evaluation of the ppar dependency of the effect. PloS one 8:e77481.

Pereira-Fernandes A, Vanparys C, Vergauwen L, Knapen D, Jorens PG, Blust R. 2014. Toxicogenomics in the 3t3-l1 cell line, a new approach for screening of obesogenic compounds. Toxicol Sci 140:352-363.

Pfaffl MW. 2001. A new mathematical model for relative quantification in real-time rt-pcr. Nucleic acids research 29:e45.

Qiang L, Wang L, Kon N, Zhao W, Lee S, Zhang Y, et al. 2012. Brown remodeling of white adipose tissue by sirt1-dependent deacetylation of ppargamma. Cell 150:620-632.

Regnier SM, El-Hashani E, Kamau W, Zhang X, Massad SL, Sargis RM. 2015. Tributyltin differentially promotes development of a phenotypically distinct adipocyte. Obesity (Silver Spring, Md In press.

Ritchie ME, Phipson B, Wu D, Hu Y, Law CW, Shi W, et al. 2015. Limma powers differential expression analyses for rna-sequencing and microarray studies. Nucleic acids research 43:e47.

Riu A, Grimaldi M, le Maire A, Bey G, Phillips K, Boulahtouf A, et al. 2011. Peroxisome proliferator-activated receptor gamma is a target for halogenated analogs of bisphenol a. Environ Health Perspect 119:1227-1232.

Rosen ED, Spiegelman BM. 2006. Adipocytes as regulators of energy balance and glucose homeostasis. Nature 444:847-853.

Schwartz MW, Seeley RJ, Zeltser LM, Drewnowski A, Ravussin E, Redman LM, et al. 2017. Obesity pathogenesis: An endocrine society scientific statement. Endocr Rev 38:267-296.

Seale P, Kajimura S, Yang W, Chin S, Rohas LM, Uldry M, et al. 2007. Transcriptional control of brown fat determination by prdm16. Cell metabolism 6:38-54.

Shoucri BM, Hung VT, Chamorro-Garcia R, Shioda T, Blumberg B. 2018. Retinoid x receptor activation during adipogenesis of female mesenchymal stem cells programs a dysfunctional adipocyte. Endocrinology 159:2863-2883.

Sidossis L, Kajimura S. 2015. Brown and beige fat in humans: Thermogenic adipocytes that control energy and glucose homeostasis. J Clin Invest 125:478-486.

Soukas A, Socci ND, Saatkamp BD, Novelli S, Friedman JM. 2001. Distinct transcriptional profiles of adipogenesis in vivo and in vitro. J Biol Chem 276:34167-34174.

Subramanian A, Narayan R, Corsello SM, Peck DD, Natoli TE, Lu X, et al. 2017. A next generation connectivity map: L1000 platform and the first 1,000,000 profiles. Cell 171:1437-1452 e1417.

Takacs ML, Abbott BD. 2007. Activation of mouse and human peroxisome proliferator-activated receptors (alpha, beta/delta, gamma) by perfluorooctanoic acid and perfluorooctane sulfonate. Toxicol Sci 95:108-117.

Temkin AM, Bowers RR, Magaletta ME, Holshouser S, Maggi A, Ciana P, et al. 2016. Effects of crude oil/dispersant mixture and dispersant components on ppargamma activity in vitro and in

vivo: Identification of dioctyl sodium sulfosuccinate (doss; cas #577-11-7) as a probable obesogen. Environ Health Perspect 124:112-119.

Timmons JA, Pedersen BK. 2009. The importance of brown adipose tissue. The New England journal of medicine 361:415-416; author reply 418-421.

Tontonoz P, Hu. E, Spiegelman BM. 1994. Stimulation of adipogenesis in fibroblasts by pparg2, a lipid-activated transcription factor. Cell 79:1147-1156.

Villanueva CJ, Vergnes L, Wang J, Drew BG, Hong C, Tu Y, et al. 2013. Adipose subtype-selective recruitment of tle3 or prdm16 by ppargamma specifies lipid storage versus thermogenic gene programs. Cell metabolism 17:423-435.

Wang H, Liu L, Lin JZ, Aprahamian TR, Farmer SR. 2016. Browning of white adipose tissue with roscovitine induces a distinct population of ucp1+ adipocytes. Cell metabolism 24:835-847.

Xiong Y, Soumillon M, Wu J, Hansen J, Hu B, van Hasselt JGC, et al. 2017. A comparison of mrna sequencing with random primed and 3'-directed libraries. Sci Rep 7:14626.

Yang X, Enerback S, Smith U. 2003. Reduced expression of foxc2 and brown adipogenic genes in human subjects with insulin resistance. Obesity research 11:1182-1191.

Zhang J, Fu M, Cui T, Xiong C, Xu K, Zhong W, et al. 2004. Selective disruption of ppargamma 2 impairs the development of adipose tissue and insulin sensitivity. Proc Natl Acad Sci U S A 101:10703-10708.

Zuriaga MA, Fuster JJ, Gokce N, Walsh K. 2017. Humans and mice display opposing patterns of "browning" gene expression in visceral and subcutaneous white adipose tissue depots. Front Cardiovasc Med 4:27.

Tables:

Table 1. Summary of experimental conditions

	3T3-L1	HUMAN PREADIPOCYTES
Exposure Period (days)	10	14
Number of times doseD	4	6
Positive Control	Rosiglitazone	Rosiglitazone
Negative Control (Vehicle)	DMSO	DMSO
Endpoint	**Test Chemicals and Concentrations (M)**	
Transcriptome Analysis	Rosiglitazone (100 nM)	NP
Lipid Accumulation	See Table S1	Rosiglitazone (4 μM) Quinoxyfen (4 μM) Tonalide (4 μM)
RT-qPCR	Rosiglitazone (1 or 20 μM) Roscovitine (2 μM) 15dPGJ2 (1 μM) TBBPA (20 μM) TPhP (10 μM)	
Cell Death		
Fatty Acid Uptake		
Mitobiogenesis		
Cell Number		
Oxygen Consumption	Quinoxyfen (10 μM) Tonalide (4 μM)	NP

NP – not performed

Table 2. Amended random forest classification results for 17 compounds suspected to be PPARγ Ligands/Modifiers.

CHEMICAL NAME	REFEFRENCE	KNOWN SOURCE/USE	PPARγ LIGAND/MODIFIER (VOTE ± 95% CI)
CHEMICALS ABOVE THE HIGHEST F1-SCORE THRESHOLD			
d-cis,trans-Allethrin	(Auerbach et al. 2016)[a]	Insecticide	0.91 ± 0.01
Tonalide	(Pereira-Fernandes et al. 2013)	Musk (fragrance)	0.90 ± 0.01
Quinoxyfen	(Auerbach et al. 2016)	Fungicide	0.90 ± 0.01
Fenthion	(Auerbach et al. 2016)	Insecticide	0.88 ± 0.01
2,4,6-Tris(tert-butyl)phenol	(Auerbach et al. 2016)	Antioxidant (industrial)	0.80 ± 0.02
Prallethrin	(Auerbach et al. 2016)	Insecticide	0.78 ± 0.02
Tebuconazole	(Auerbach et al. 2016)	Fungicide	0.78 ± 0.02
Fludioxonil	(Auerbach et al. 2016)	Fungicide	0.77 ± 0.02
Tris(1,3-dichloro-2-propyl) phosphate	(Fang et al. 2015b)	Flame retardant	0.76 ± 0.02
Cyazofamid	(Auerbach et al. 2016)	Pesticide	0.72 ± 0.02
Perfluorooctanoic acid	(Takacs and Abbott 2007)	Fluorosurfactant	0.59 ± 0.02
Triphenyl phosphite	(Fang et al. 2015a)	Pesticide	0.57 ± 0.02
Tris(1-chloro-2-propyl) phosphate	(Fang et al. 2015b)	Flame retardant	0.54 ± 0.02
CHEMICALS BELOW THE HIGHEST F1-SCORE THRESHOLD			
Triphenylphosphine oxide	(Hiromori et al. 2016)	Crystallizing aid, byproduct	0.49 ± 0.02
Diphenyl phosphate	(Cano-Sancho et al. 2017)	Metabolite of TPhP	0.47 ± 0.02
Dioctyl sulfosuccinate sodium	(Temkin et al. 2016)	Surfactant	0.41 ± 0.02
Perfluorooctanesulfonic acid	(Takacs and Abbott 2007)	Fluorosurfactant	0.40 ± 0.02

[a] We used the ToxPi designed to identify chemicals in the ToxCast dataset that are likely to be PPARγ ligands/modifiers.

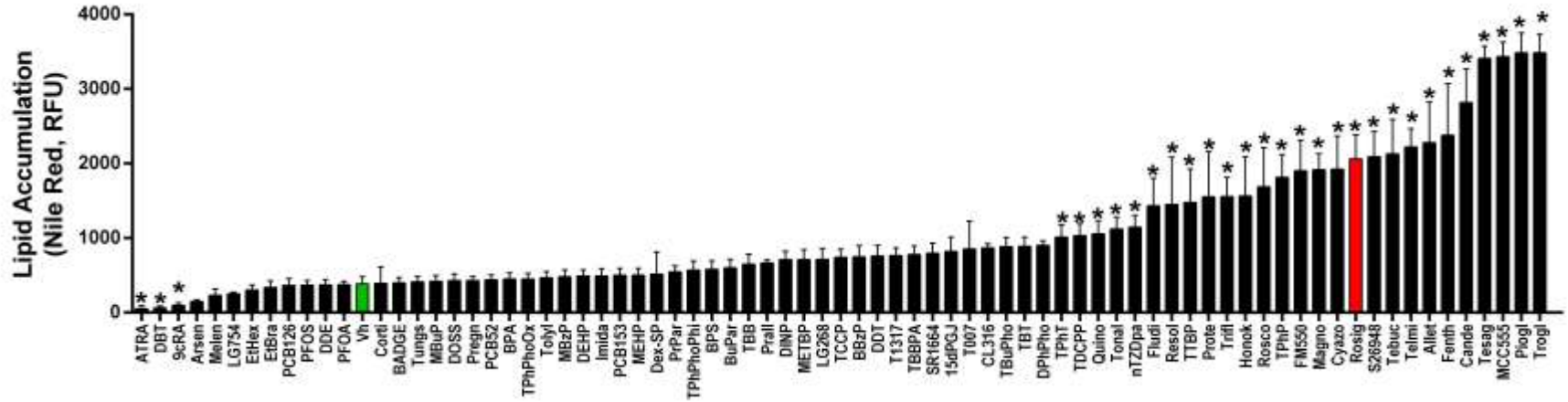

Figure 1. Lipid accumulation in differentiated and treated 3T3-L1 pre-adipocytes.
Confluent 3T3 L1 cells were differentiated using a standard hormone cocktail for 10 days. During differentiation, cells were treated with vehicle (Vh, 0.2% DMSO, final concentration), rosiglitazone (positive control, 100 nM) or test chemical (**Table S1**). On days 3, 5, and 7 of differentiation, the medium was replaced and the cultures re-dosed. Following 10 days of differentiation and dosing, cells were analyzed for lipid accumulation by Nile Red staining. Data are presented as mean ± SE (n=4). Statistically different from Vh-treated (highlighted in green) (*$p<0.05$, ANOVA, Dunnett's).

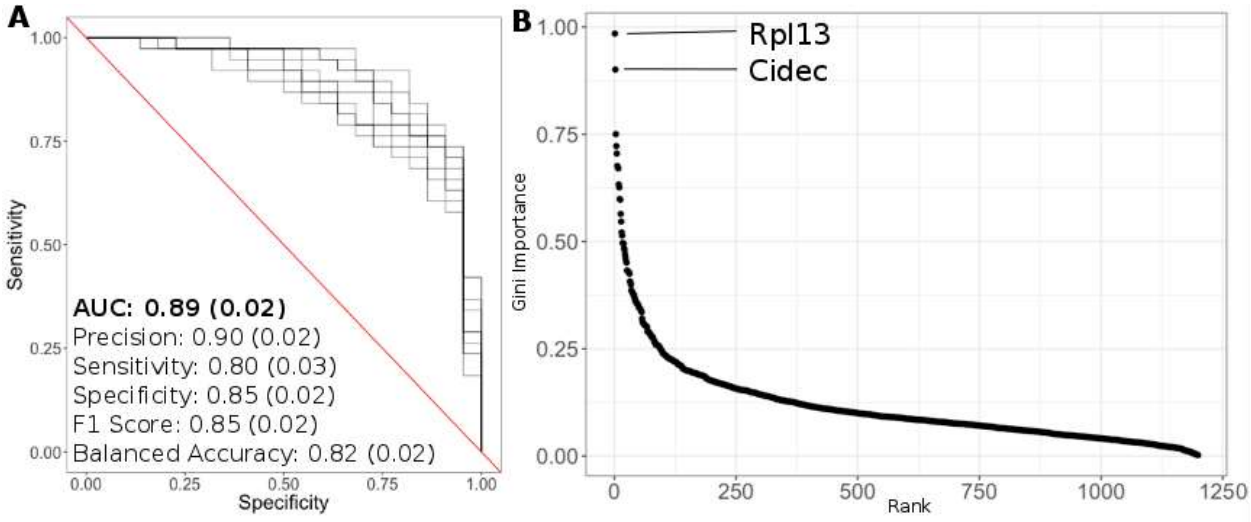

Figure 2. Amended random forest classification performance and gene importance of final classification model.
(A) Performance of random forest classification procedure based on 10-fold cross validation. **(B)** Gini Importance versus ranking of genes used in the final random forest model. The names of the top 2 genes are highlighted. Compound-specific gene expression of *Rpl13* and *Cidec* are shown in **Figure S4**.

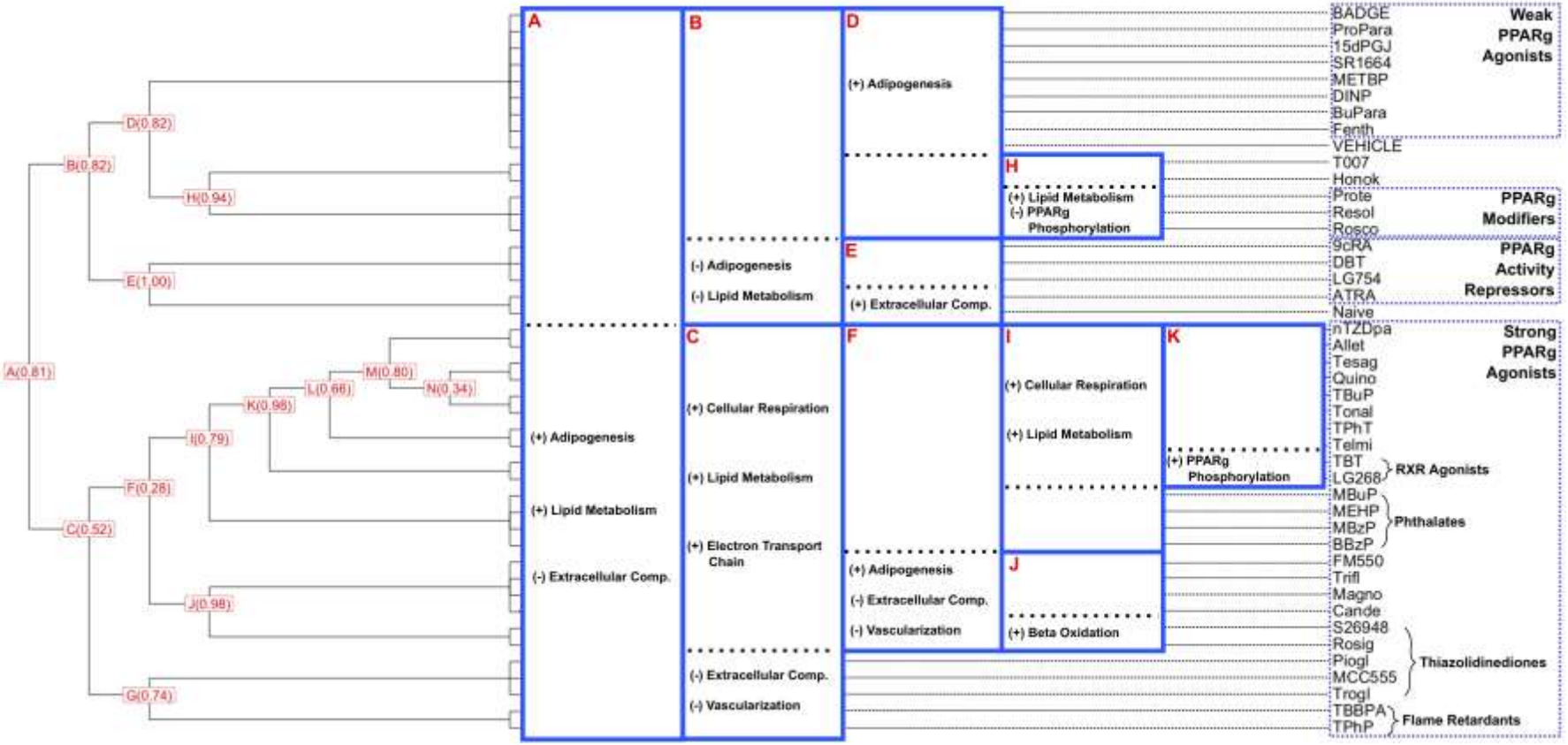

Figure 3. Chemical taxonomy of PPARγ ligands/modifers based on K2 clustering of the 3'DGE data.
The dendrogram shows the taxonomy-driven hierarchical grouping of test chemical exposures of 3T3-L1 cells or naïve pre-adipocytes. Each split is labeled with a letter, and the proportion of gene-level bootstraps which produced the resulting split is shown. Highlights of hyper-enrichment of gene ontology (GO) biological processes are shown.

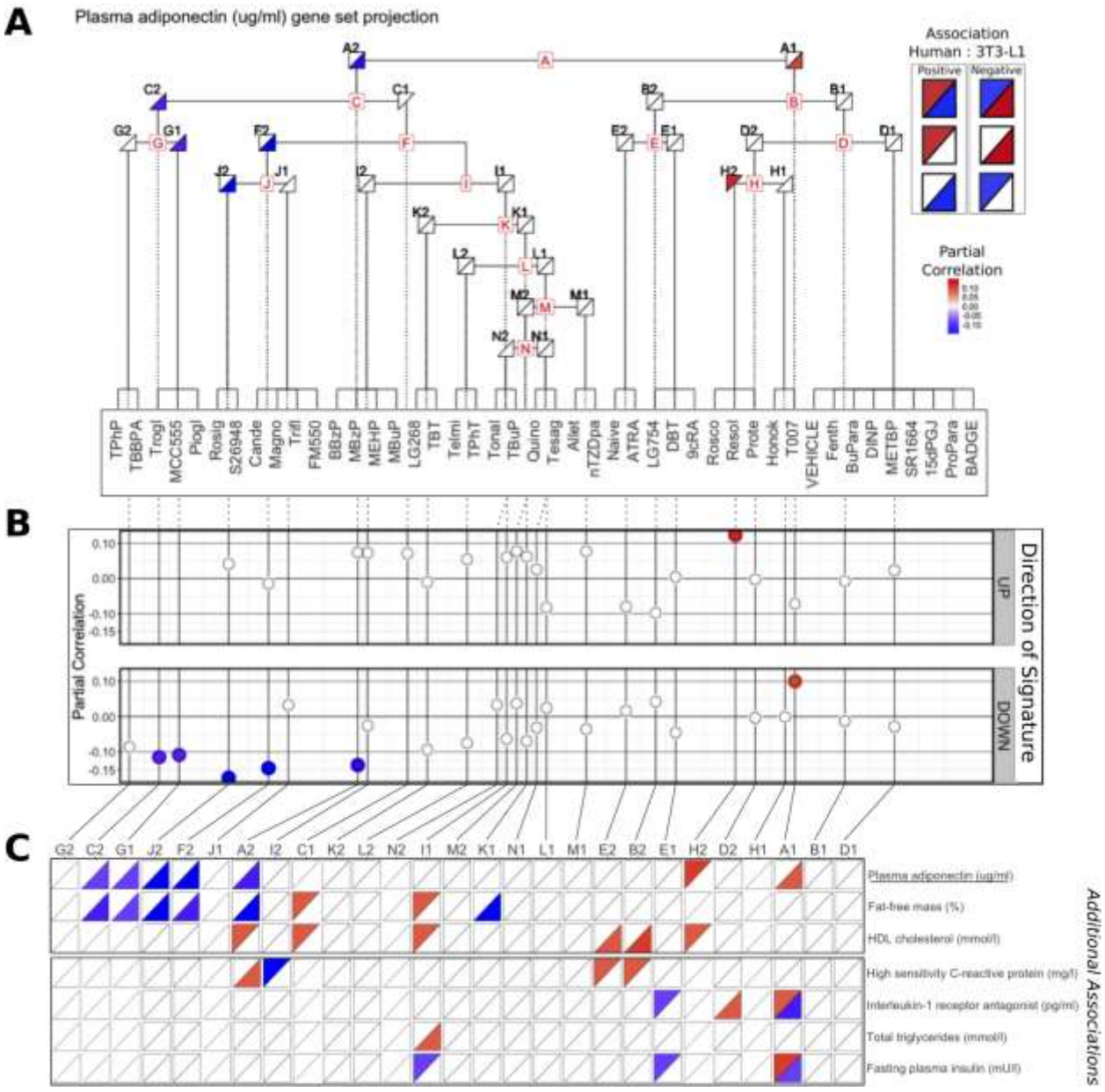

Figure 4. Associations between plasma adiponectin levels and projections of the 3T3-L1 derived chemical taxonomy gene signatures onto human adipose tissue gene expression.
(A) Each adjoined triangle in the dendrogram denotes a set of genes derived from the 3T3-L1 data, either up-regulated (left) or down-regulated (right) at a given node. Triangles are colored according to the direction of the partial correlation of the projection of these gene sets with plasma adiponectin levels. Interpretation of these associations is in the key on the upper right. All colored triangles reach a significance threshold of FDR Q-value < 0.10. **(B)** Plots of the partial correlation measurements for gene set projections and plasma adiponectin levels. The top and bottom plots are indicative of gene sets that are either up- or down-regulated in a particular sub-group, respectively. All colored points reach a significance threshold of FDR Q-value <

0.10, as in (A). **(C)** Results of all partial correlation analyses of projection of taxonomy gene sets with clinical measurements with at least one comparison reaching significance, FDR Q-value < 0.10. The interpretation of these associations is the same as in (A).

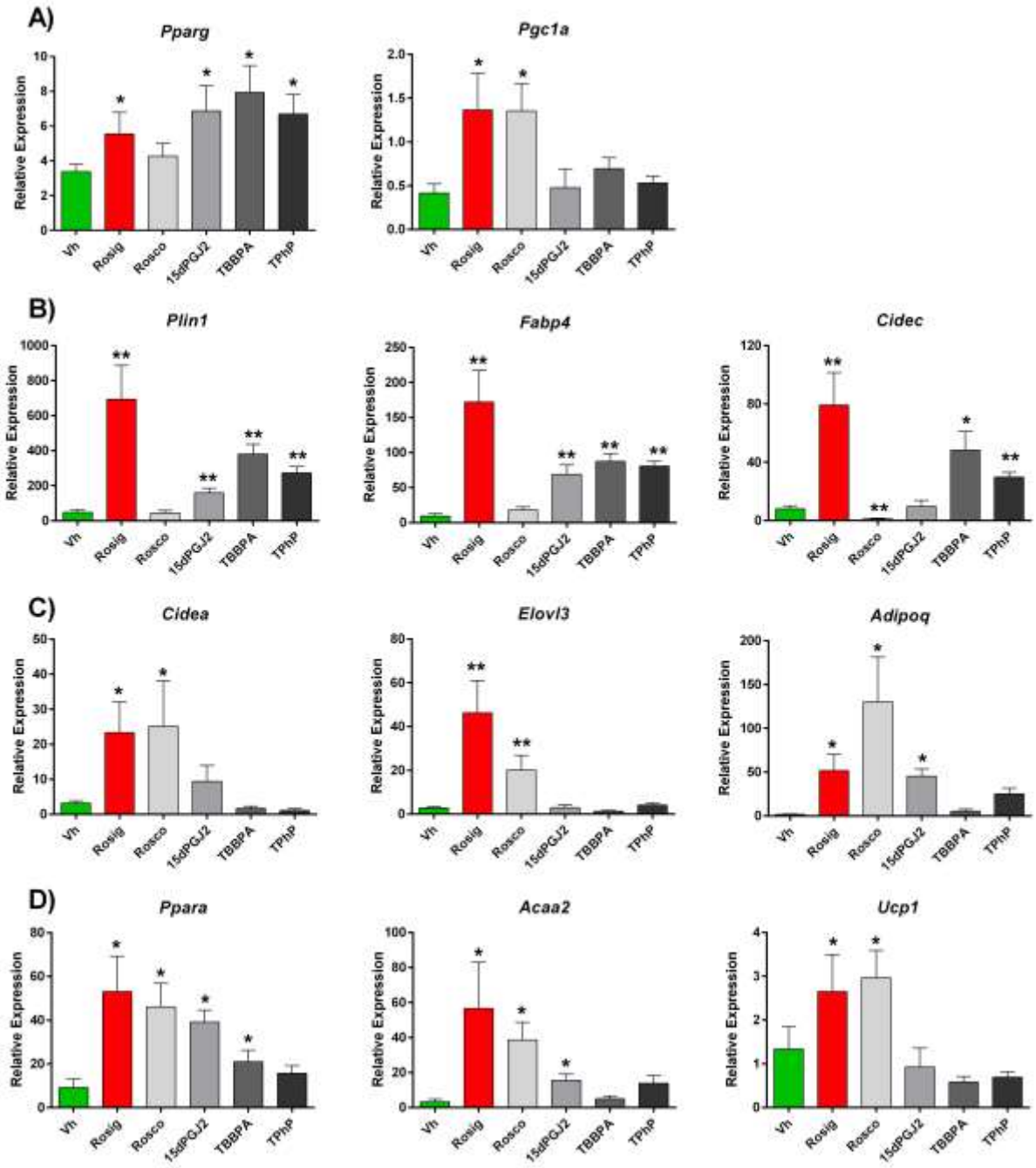

Figure 5. White and brite gene expression in differentiated and treated 3T3-L1 adipocytes. Confluent 3T3 L1 cells were differentiated using a standard hormone cocktail for 10 days. During differentiation, cells were treated with vehicle (Vh, 0.2% DMSO, final concentration), rosiglitazone (Rosig, 1 μM), roscovitine (Rosco, 2 μM), 15dPGJ2 (1 μM), TBBPA (20 μM) and TPhP (10 μM). On days 3, 5, and 7 of differentiation, the adipocyte maintenance medium was replaced and the cultures re-dosed. Following 10 days of differentiation and dosing, cells were analyzed for gene expression by RT-qPCR. **(A)** PPARγ and coregulator expression. **(B)** Genes

related to white adipogenesis. **(C)** Genes related to brite adipogenesis. **(D)** Genes related to mitochondrial biogenesis and energy expenditure. Data are presented as mean ± SE of n=4 independent experiments. Statistically different from Vh-treated (highlighted in green) (*p<0.05, **p<0.01, ANOVA, Dunnett's).

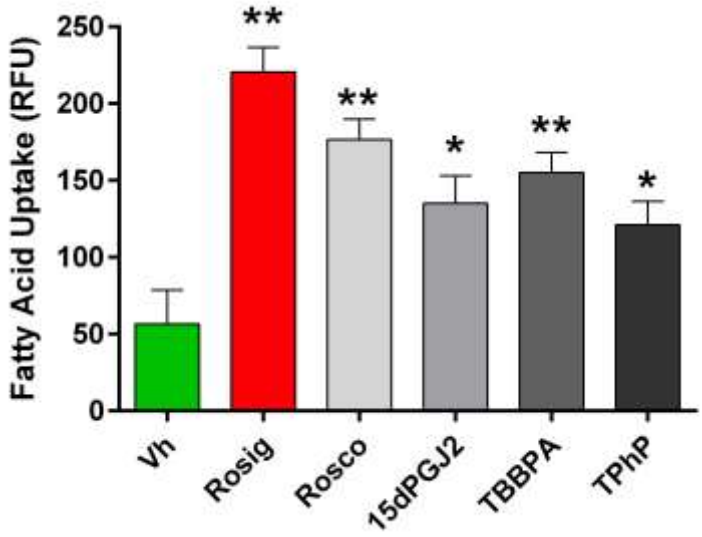

Figure 6. Fatty acid uptake in differentiated and treated 3T3-L1 adipocytes. Differentiation and dosing were carried out as described in Figure 5. Following 10 days of differentiation, fatty acid uptake was analyzed using a dodecanoic acid fluorescent fatty acid substrate. Data are presented as means ± SE (n=4). Statistically different from Vh-treated (highlighted in green) (*$p<0.05$, **$p<0.01$, ANOVA, Dunnett's).

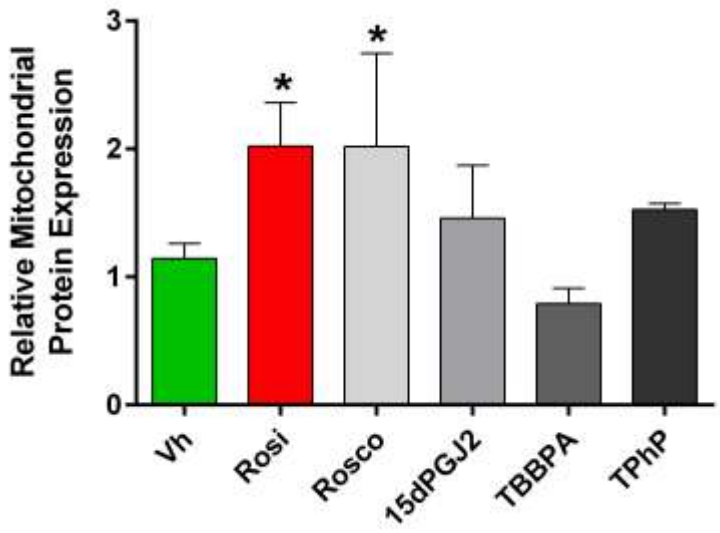

Figure 7. Mitochondrial biogenesis in differentiated and treated 3T3-L1 adipocytes. Differentiation and dosing were carried out as described in Figure 5. Following 10 days of differentiation, mitochondrial biogenesis was analyzed by measuring mitochondria-specific proteins. Vehicle, Rosig and TPhP data have been published previously (Kim et al. 2020). Data are presented as means ± SE (n=4). Statistically different from Vh-treated (highlighted in green) (*$p<0.05$, ANOVA, Dunnett's).

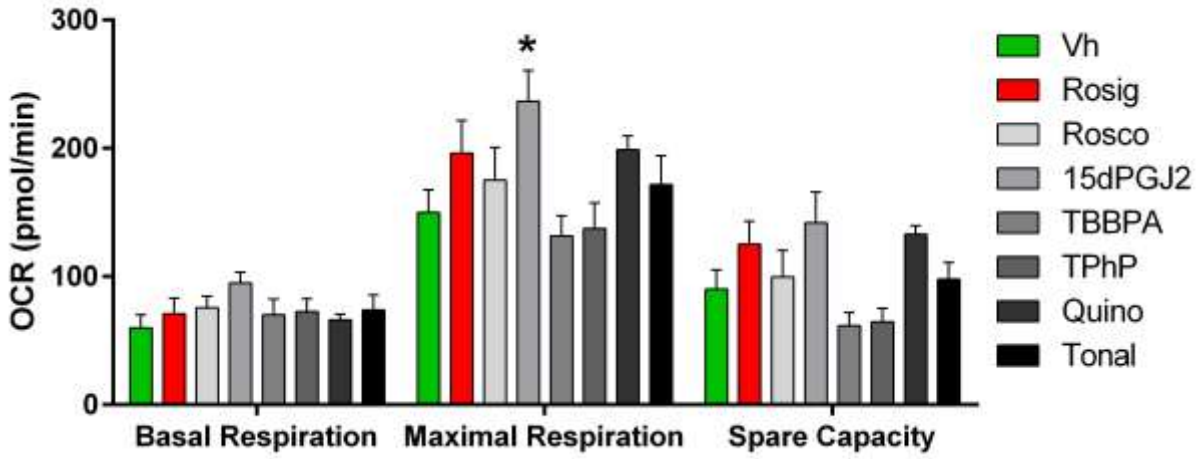

Figure 8. Cellular respiration in differentiated and treated 3T3-L1 adipocytes. Differentiation and dosing were carried out as described in Figure 5, with the exception of Rosig (20 µM). Following 10 days of differentiation, mitochondrial respiration was analyzed by Seahorse Assay. Vehicle, Rosig and TPhP data have been published previously (Kim et al. 2020). Data are presented as means ± SE (n=4). Statistically different from Vh-treated (highlighted in green) (*$p<0.05$, ANOVA, Dunnett's).

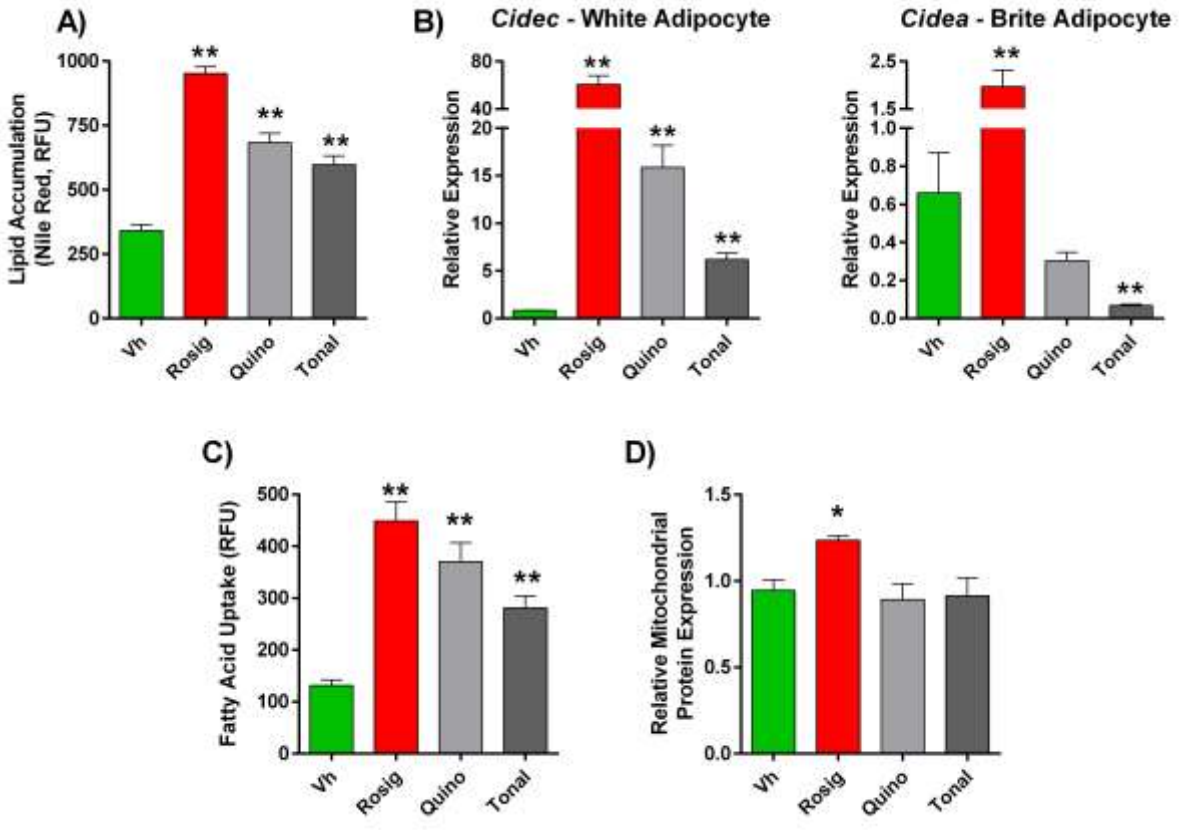

Figure 9. Tonalide and quinoxyfen induce white, but not brite, adipogenesis in 3T3-L1 pre-adipocytes.

Confluent 3T3 L1 cells were differentiated using a standard hormone cocktail for 10 days. During differentiation, cells were treated with vehicle (Vh, 0.2% DMSO, final concentration), rosiglitazone (Rosig, 1 μM), quinoxyfen (Quino, 10 μM) or tonalide (Tonal, 4 μM). On days 3, 5, and 7 of differentiation, the adipocyte maintenance medium was replaced and the cultures re-dosed. Following 10 days of differentiation and dosing, cultures were analyzed for **(A)** adipocyte differentiation, **(B)** white (*Cidec*) and brite (*Cidea*) gene expression, **(C)** fatty acid uptake, and **(D)** mitochondrial biogenesis. Data are presented as means ± SE (n=4). Statistically different from Vh-treated (highlighted in green) (*$p<0.05$, ANOVA, Dunnett's).

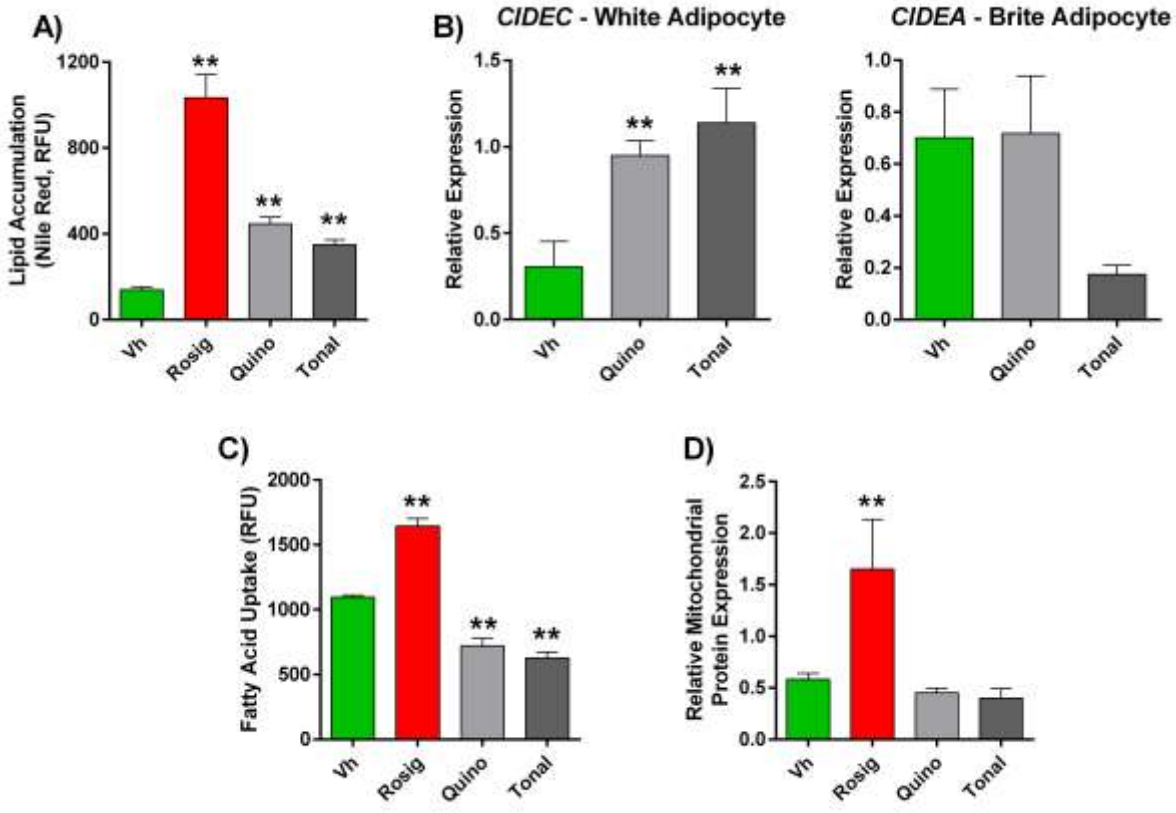

Figure 10. Tonalide and quinoxyfen induce white, but not brite, adipogenesis in primary human adipocytes.

Confluent primary human preadipocytes were differentiated using a standard hormone cocktail for 14 days. During differentiation, cells were treated with vehicle (Vh, 0.1% DMSO, final concentration), rosiglitazone (Rosig, 4 μM), quinoxyfen (Quino, 4 μM) or tonalide (4 μM). On days 3, 5, 7, 10, and 12 of differentiation, the medium was replace and the cultures re-dosed. Following 14 days of differentiation and dosing, cultures were analyzed for **(A)** adipocyte differentiation, **(B)** white (*Cidec*) and brite (*Cidea*) gene expression, **(C)** fatty acid uptake, and **(D)** mitochondrial biogenesis. Data are presented as mean ± SE (n=3, each n is from adipocytes from an individual). Statistically different from Vh-treated (highlighted in green) (*$p<0.05$, ANOVA, Dunnett's).